

# Evolution and mechanism of contact resistance of copper–aluminum electrical connectors in lithium-ion power batteries

Junlian Ge<sup>1</sup> , Jialin Zhu<sup>2</sup>, Biao Ge<sup>1</sup> , Leon Sandforth<sup>3</sup> , Junying Min<sup>4\*</sup> 

<sup>1</sup> School of Mechanical Engineering, Tongji University, Shanghai 201804, China.

<sup>2</sup> Hefei Gotion High-Tech Power Energy Co. Ltd., Hefei 230041, China.

<sup>3</sup> Chair for Electrical Energy Storage Systems, Institute for Photovoltaics (IPV), University of Stuttgart, Pfaffenwaldring 47, 70569 Stuttgart, Germany.

<sup>4</sup> College of Automotive and Energy Engineering, Tongji University, Shanghai 201804, China.

## Abstract

This study investigates the sensitivity of factors influencing the contact resistance and reliability assessment of bolted copper–aluminum electrical connectors. Through continuous energized dynamic testing, the temporal evolution of the contact resistance and temperature of the contact area were monitored throughout the experiment. In conjunction with observations of contact surface morphology and microstructural composition analysis, the intrinsic mechanisms underlying anomalous changes in contact resistance were explored in depth. The results indicated that, during continuous current flow, the contact resistance of aluminum busbar assemblies without plating exhibited an “initially low → rapid increase → gradual stabilization” pattern, whereas nickel-plated aluminum assemblies maintained stable resistance. Quantitatively, the contact resistance of the nickel-plated group remained at approximately 15  $\mu\Omega$ , while that of the bare aluminum group rose to 400–750  $\mu\Omega$ . The evolution of the contact interface was asymmetric, with the dynamic growth of the oxide layer on the aluminum surface being the dominant mechanism increasing resistance. Moreover, the aluminum coating significantly reduced contact resistance and enhanced connection reliability.

**Keywords:** lithium-ion power batteries, electrical connection, contact resistance, contact mechanism

## 1. Introduction

In automotive power lithium-ion batteries, numerous electrical connectors are integrated within the system, serving as critical pathways for energy transfer and signal communication. The contact reliability at these interfaces directly affects the operational stability of both the lithium-ion cells and the vehicle’s powertrain system. Among the various failure modes of electrical connectors, anomalous increases in contact resistance represent

one of the most frequent and impactful failure phenomena (Kolmer et al., 2022; Song et al., 2019). Excessive contact resistance under high-current conditions can result in a rapid temperature rise in the contact region, potentially exceeding safe operational thresholds. The hazards associated with such localized overheating are progressive: they not only accelerate the aging and degradation of the conductive materials and surrounding insulating components, significantly reducing the service life of the connectors and battery modules, but if left un-

\* Corresponding author

Authors' e-mails: [gejunlian@tongji.edu.cn](mailto:gejunlian@tongji.edu.cn), [zhujialin@gotion.com.cn](mailto:zhujialin@gotion.com.cn), [gebiao@tongji.edu.cn](mailto:gebiao@tongji.edu.cn), [leon.sandforth2@gmail.com](mailto:leon.sandforth2@gmail.com), [junying.min@tongji.edu.cn](mailto:junying.min@tongji.edu.cn)

ORCID IDs: 0009-0005-2542-5122 (J. Ge), 0009-0009-7537-0552 (B. Ge), 0009-0004-3839-927X (L. Sandforth), 0000-0002-1754-6259 (J. Min)

Received: 15.04.2026, accepted: 17.05.2026, published: 26.06.2026

© 2026 Authors. This is an open access publication, which can be used, distributed and reproduced in any medium according to the Creative Commons CC BY 4.0 License requiring that the original work has been properly cited.

controlled, may also lead to severe safety failures such as electrical breakdown and insulation failure, thereby posing a substantial risk to the overall safety of the power battery system (Song et al., 2025; Taheri et al., 2011).

To address the aforementioned thermal failure issues, the design of electrical connectors aims to optimize the contact interface to achieve low and stable contact resistance, thereby ensuring that the maximum temperature within the contact region remains below the specified limit while maintaining performance stability under long-term operational conditions (Kalich et al., 2022; Khayam et al., 2017). Previous studies have identified that the factors influencing contact resistance in electrical connectors primarily include the base material, surface plating material, plating thickness, and contact force. Surface plating can reduce contact resistance by enhancing the electrical conductivity of the interface, preventing oxidation of the base material, or inhibiting interdiffusion between dissimilar connector materials (Khayam et al., 2014; Tian, 2019; Wu, 2017; Zhu, 2023). A sufficiently thick plating layer can effectively prevent exposure of the underlying metal, avoiding resistance increases due to base material oxidation, and can preserve the integrity and functionality of the coating even after minor wear (Bao et al., 2018; Feng et al., 2021; Hu et al., 2019; Zhang Y. et al., 2019). Contact force regulates the level of contact resistance by affecting the deformation of contact spots and the real contact area (Alderete et al., 2023; Huang et al., 2022; Zhang C. et al., 2022; Zhi, 2016).

Regarding the selection of base materials, copper has long been the preferred choice for electrical connectors due to its excellent electrical conductivity. However, with the increasing demands for lightweight design and cost reduction in automotive battery systems, aluminum, which is characterized by low density and a significant cost advantage, has gradually been introduced to partially replace copper as a connector material in power battery electrical systems (Runde, 2019). Nevertheless, the aluminum surface readily forms a poorly conductive oxide layer that is difficult to fully break during mechanical assembly, resulting in copper–aluminum connectors exhibiting higher contact resistance and generally

lower long-term reliability compared to copper–copper connectors. Existing research and relevant standards for copper–aluminum connectors have predominantly focused on high-voltage power transmission and cable connections, while studies on key factors influencing contact resistance and reliability testing of copper–aluminum connectors under the low-voltage, high-current conditions typical of automotive lithium-ion battery systems remain limited (Elkjaer et al., 2022; Slade, 2017).

Therefore, focusing on bolted copper–aluminum electrical connectors, this study first carried out a sensitivity analysis of the factors influencing contact resistance through static contact resistance measurements and variance analysis. Based on these results, the primary influencing factors were identified, and continuous current dynamic tests under different current levels were performed to monitor the temporal evolution of both contact resistance and the temperature of the contact region, thereby assessing the stability and reliability of the connectors. Complementary observations of the contact interface morphology and compositional analysis were carried out to reveal the underlying mechanisms driving variations in contact resistance. The findings of this study aim to provide a theoretical basis for the high-reliability design of electrical connection systems in automotive lithium-ion batteries.

## 2. Materials and methods

### 2.1. Materials

This study primarily carried out performance and characterization tests on plated copper busbars, plated aluminum busbars, and bare aluminum busbars used in lithium-ion automotive battery system electrical connectors. The specific sample types are shown in Table 1. Among which, “O” condition aluminum refers to aluminum that has undergone full annealing, resulting in the lowest strength and a generally softer texture; “H” condition aluminum refers to aluminum that has undergone work hardening, resulting in higher strength and greater hardness.

**Table 1.** Sample types

Base material	Type of plating	Thickness of plating	Aluminum busbar state
Copper	tin plating	6 $\mu\text{m}$	–
	tin plating with nickel underlayer	5 $\mu\text{m}$	–
		8 $\mu\text{m}$	–
Aluminum	without plating	–	O condition
			H condition
	nickel plating	same thickness	O condition
			H condition

## 2.2. Experimental methods

Contact resistance measurements of the electrical connectors were carried out using the four-wire method to eliminate the influence of lead and probe resistance and to enable precise micro-ohm-level determination of contact resistance. Static contact resistance tests were first performed to quantify resistance levels under different factor conditions, and variance analysis was employed to identify key influencing factors. Based on these results, dynamic current tests were further carried out to evaluate the contact reliability and potential thermal risks of the interface under continuous current conditions. The experimental design for the static tests, summarizing all combinations of factors investigated, is presented in Table 2. During the dynamic test, the samples were placed inside an extruded polystyrene insulation box, with the contact resistance and the adjacent surface temperature monitored in real time. The temperature was measured using thermocouples, which were fixed in position near the contact area with high-temperature-resistant insulating tape throughout the dynamic testing.

The copper and aluminum busbars were mechanically connected using M6 bolts. Prior to assembly, the contact surfaces were cleaned with ethanol to remove any surface oxides or contaminants. The bolts were tightened using a calibrated torque wrench to a specified torque. Except for the contact force test, all copper–aluminum connectors were assembled with a tightening torque of 8 N·m. The static test current was set to 100 A, while dynamic tests were carried out at 100 A, 200 A, and 300 A. The test current was set based on the actual operating current encountered in the battery pack application. For plated aluminum busbar assem-

blies, the test duration under the 100 A, 200 A, and 300 A conditions was 1 h. For bare aluminum busbar assemblies, the duration was 1 h under the 100 A and 200 A conditions, while under the 300 A condition, the test duration was shortened to 45 min because the contact resistance stabilized more quickly and the surface temperature approached the insulation box limit.

To research the localized wear characteristics and chemical evolution of the contact interface during current flow, the surface morphology and elemental composition of copper–bare aluminum samples were compared before and after dynamic testing. Sampling locations for surface morphology observation and X-ray photoelectron spectroscopy (XPS) analysis were selected around the via areas, enabling targeted examination of surface morphology and chemical composition evolution. These analyses revealed the nucleation and expansion of conductive spots, the degradation and regeneration of surface films, and their impact on electrical performance.

## 3. Contact resistance test results

### 3.1. Sensitivity analysis of factors influencing contact resistance

Figure 1 presents the results of static contact resistance measurements obtained under the controlled variable approach, and the corresponding one-way analysis of variance (ANOVA) results are shown in Table 3. The ANOVA results indicate that the F-values for sample hardness, aluminum busbar plating, and contact force all exceed their respective critical F-values ( $F_{crit}$ ), and the corresponding P-values are below the predetermined significance level ( $\alpha = 0.05$ ).

**Table 2.** Experimental design for static tests

ID	Type of copper busbar plating	Thickness of copper busbar plating [ $\mu\text{m}$ ]	Aluminum busbar state	Aluminum busbar plating	Contact force [N·m]
1	tin plating with nickel underlayer	5	O condition	nickel plating	8
2	tin plating	6	O condition	nickel plating	8
3	tin plating with nickel underlayer	8	O condition	nickel plating	8
4	tin plating with nickel underlayer	5	H condition	nickel plating	8
5	tin plating with nickel underlayer	5	O condition	without plating	8
6	tin plating with nickel underlayer	5	O condition	nickel plating	4 8 12
7	tin plating with nickel underlayer	5	O condition	without plating	4 8 12

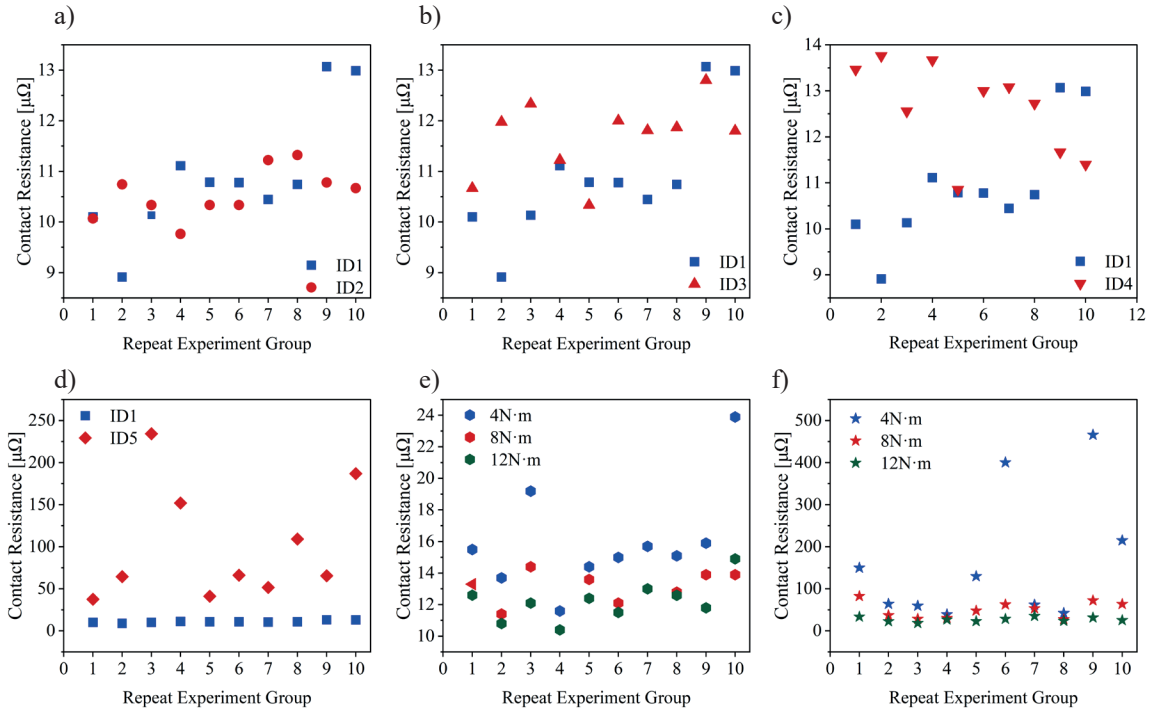


**Fig. 1.** Static contact resistance measurement results: a) copper busbar plating; b) plating thickness; c) sample hardness; d) aluminum busbar plating; e) contact force (plated aluminum busbar); f) contact force (bare aluminum busbar)

**Table 3.** ANOVA results

Potential influencing factors	Analyzed groups' IDs	<i>F</i>	<i>P</i> values	<i>F<sub>crit</sub></i>
Type of copper busbar plating	1, 2	1.84	$1.86 \times 10^{-1}$	4.19
Thickness of copper busbar plating	1, 3	2.67	$1.13 \times 10^{-1}$	4.19
Sample hardness	1, 4	8.27	$8.78 \times 10^{-3}$	4.19
Aluminum busbar plating	1, 5	14.3	$1.17 \times 10^{-3}$	4.35
Contact force (nickel-plated aluminum groups)	6	5.78	$7.06 \times 10^{-3}$	3.23
Contact force (bare aluminum groups)	7	8.58	$9.98 \times 10^{-4}$	3.28

These findings demonstrate that aluminum busbar plating, contact force, and sample hardness are all significant factors affecting the contact resistance of copper–aluminum electrical connectors. Furthermore, based on the relative magnitudes of the *F*-values and *P*-values, aluminum busbar plating is identified as the most influential factor on contact resistance. Consequently, subsequent dynamic tests focused on evaluating and comparing the electrical connection reliability of copper–nickel-plated aluminum groups versus copper–bare aluminum groups.

### 3.2. Dynamic behavior of contact resistance

Figure 2 presents the results of the dynamic tests. For the electrical connection interface composed of a bare

aluminum busbar and a copper busbar, the repeat tests showed that the contact resistance curves exhibited significant variability over time. While the overall macroscopic trend was roughly similar, the specific resistance values displayed considerable dispersion. As shown in Fig. 2a, the contact resistance of the bare aluminum busbar assemblies increased markedly during the dynamic testing and gradually stabilized over time. The electrical performance of the contact interface deteriorates under current load, indicating weak conductive stability. Regarding the temperature rise characteristics (Fig. 2b), the sample temperature increased significantly with the increasing current. Under a 100 A current, the temperature remained within the safe range; however, at 200 A and 300 A, the temperature rose rapidly and exceeded 80°C, reaching the specified threshold and posing an overheating risk when operating in a battery pack.

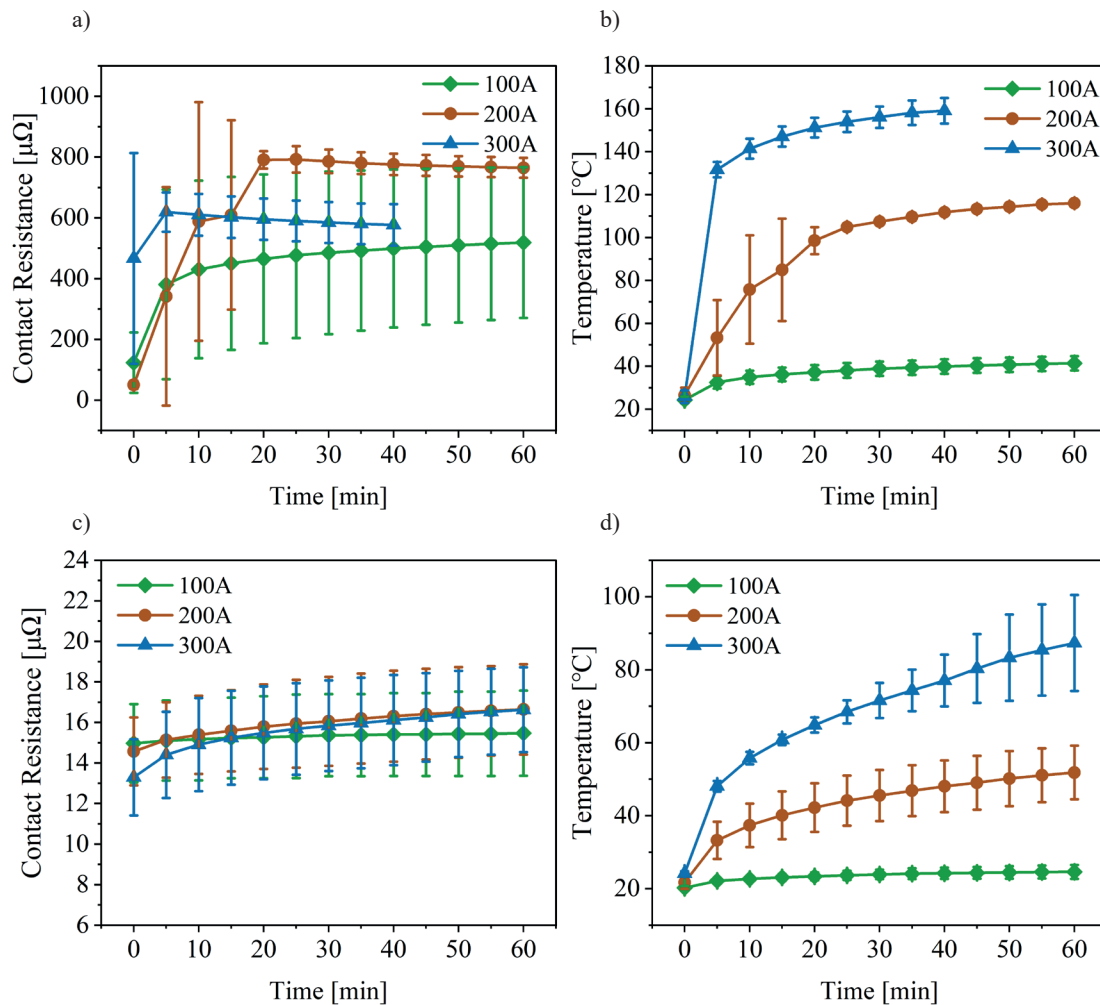


**Fig. 2.** Dynamic test results: a) contact resistance variation of the bare aluminum busbar assembly; b) surface temperature variation of the bare aluminum busbar assembly; c) contact resistance variation of the nickel-plated aluminum busbar assembly; d) surface temperature variation of the nickel-plated aluminum busbar assembly

In contrast, as shown in Fig. 2c, the contact resistance of the nickel-plated aluminum busbar assemblies remained stable throughout the entire testing, and no significant resistance degradation was observed despite the increasing current or prolonged energization time. In terms of temperature rise (Fig. 2d), the sample temperature increased with the current, yet remained within the safe operating range under 100 A and 200 A. At 300 A, the temperature reached the designated safety threshold. Taken together, these results indicate that bare aluminum busbar groups exhibit poor electrothermal stability and reliability under continuous current load. Nickel plating of the aluminum busbar effectively maintained the stability of the contact interface. Nevertheless, changes in contact resistance alone cannot serve as the sole criterion for long-term electrical connection performance. Limiting the operating current and improving heat dissipation are also critical measures for enhancing the reliability of electrical connections.

## 4. Mechanism of contact resistance evolution

### 4.1. Changes in surface microstructure and surface chemical composition

Based on the observation images and the corresponding surface roughness measurements of the sample surfaces before and after dynamic testing (Fig. 3 and 4), the morphologies of the aluminum busbars exhibited only minor changes. In contrast, the copper busbars showed evident contact marks after testing: the overall height of the surface microstructure decreased significantly and the surface roughness of the copper busbars decreased substantially, with a reduction of approximately 70%. These results indicated that morphological evolution of the contact interface primarily occurred on the copper busbars. This asymmetric surface evolution is attributed to the hardness difference between aluminum and tin. Under the applied contact force, deformation mainly occurred on the softer tin-plated copper surface.

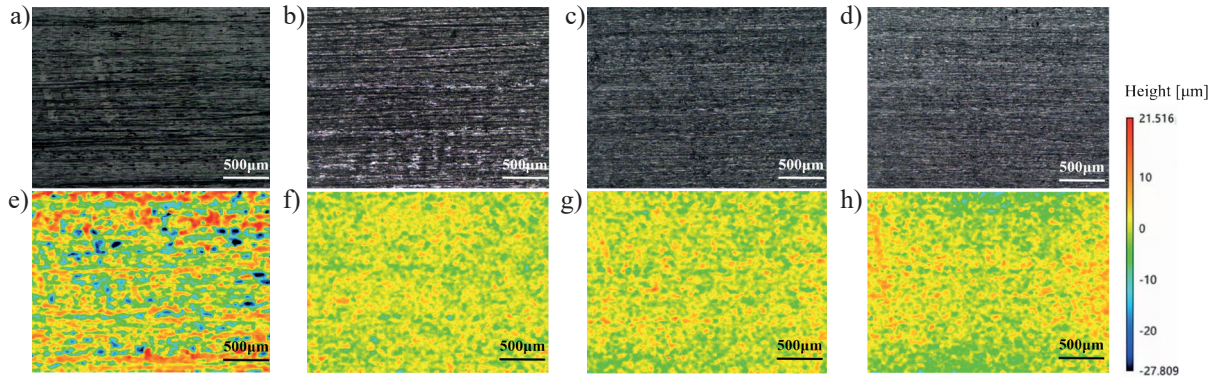


**Fig. 3.** Surface morphology observations of samples: a, e) surface height distribution of the copper busbar before dynamic testing; b, f) surface height distribution of the copper busbar after dynamic testing; c, g) surface height distribution of the aluminum busbar before dynamic testing; d, h) surface height distribution of the aluminum busbar after dynamic testing

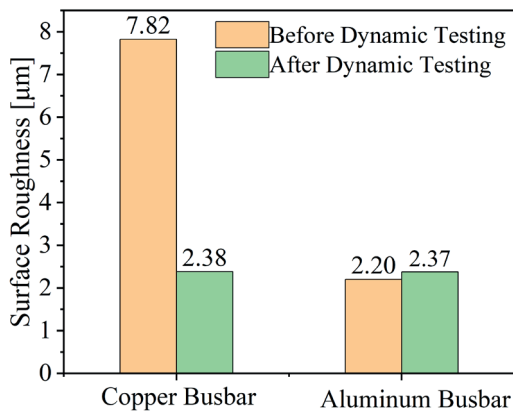


**Fig. 4.** Surface roughness variations of samples

The relative elemental composition of the sample surfaces measured by X-ray photoelectron spectroscopy (XPS) is presented in Figs. 5a and 5b. The primary elements on the tin-plated copper busbar surface were C, O, and Sn, with only minor changes in the relative concentrations before and after the dynamic testing, indicating overall stability. In contrast, the elemental composition of the aluminum busbar surface underwent significant changes during the dynamic testing: C, O, and Al remained the dominant elements, but the relative content of C decreased notably from 77.4% to 63.4%, while the relative contents of O and Al increased markedly from 19.4% to 30.5% and from 3.2% to 6.1%, respectively.

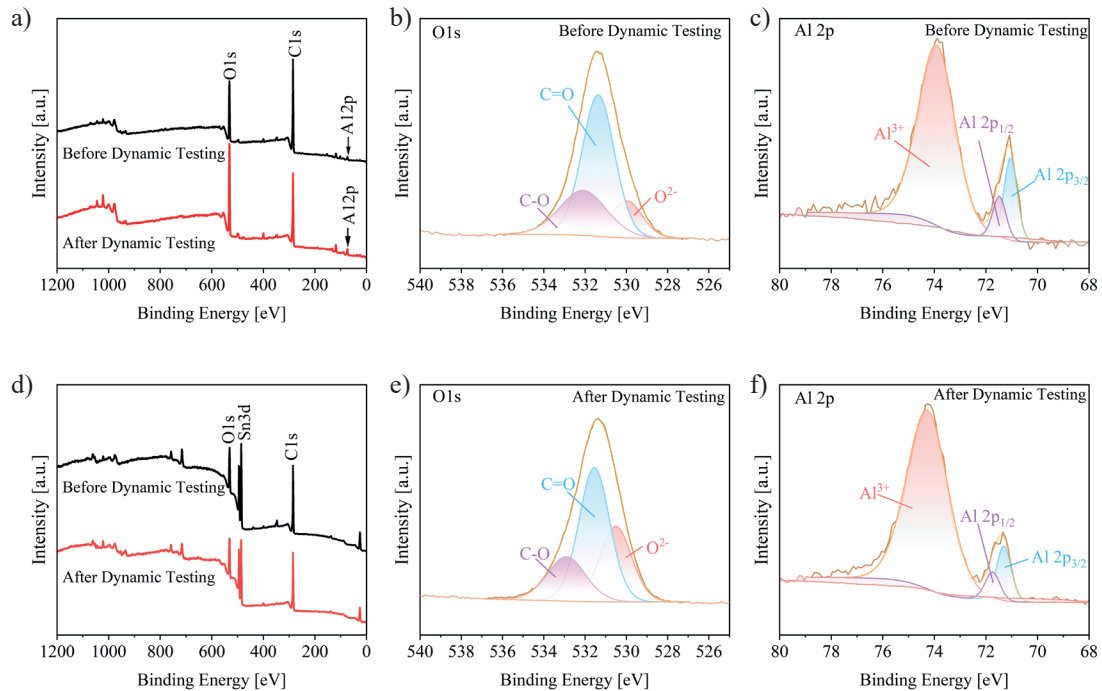


**Fig. 5.** XPS test results: a, b) elemental composition changes on aluminum and copper busbar surfaces before and after dynamic testing; c, d) high-resolution XPS fitting results of oxygen on the aluminum busbar surface before and after dynamic testing; e, f) high-resolution XPS fitting results of aluminum on the aluminum busbar surface before and after dynamic testing

Further analysis of the high-resolution XPS spectra of Al and O on the aluminum surface (Fig. 5c–5e) indicated that aluminum on the surface primarily existed in oxidized states, suggesting the formation of a relatively stable oxide layer. Under dynamic testing conditions, the evolution of the surface chemistry at the contact interface mainly occurred on the aluminum busbar, manifested as an increase in surface oxidation. Meanwhile, the reduction in carbon content may be associated with localized electro-thermal coupling during testing, which caused thermal decomposition or volatilization of organic contaminants originally adsorbed on the aluminum surface, thereby exposing more underlying aluminum and its oxides.

#### 4.2. Verification of the dominant mechanism in contact resistance evolution

A set of cross-comparison experiments was designed and carried out to verify that the surface composition changes in the aluminum busbars is the primary factor driving changes in contact resistance in copper–

aluminum electrical connectors. Specifically, the aluminum busbars from the two dynamically tested assemblies (copper busbar–nickel-plated aluminum busbar, and copper busbar–bare aluminum busbar) were interchanged, and dynamic testing was performed to compare the trends in electrical contact performance under an identical copper or aluminum busbar.

As shown in Figure 6, when using the same bare or nickel-plated aluminum busbar, the contact resistance and temperature rise curves exhibited very similar trends and comparable stabilized values throughout the testing, even when paired with different copper busbars. This indicates that the surface condition of the aluminum busbar has a decisive influence on the electrical contact behavior at the interface. Conversely, when the copper busbar was kept the same but the aluminum busbar differed, the contact resistance and temperature rise curves showed significant differences. This comparison directly demonstrates that changes in the copper busbar surface morphology are not the primary cause of variations in contact resistance; rather, the variations are rooted in differences in the surface condition of the aluminum busbar.

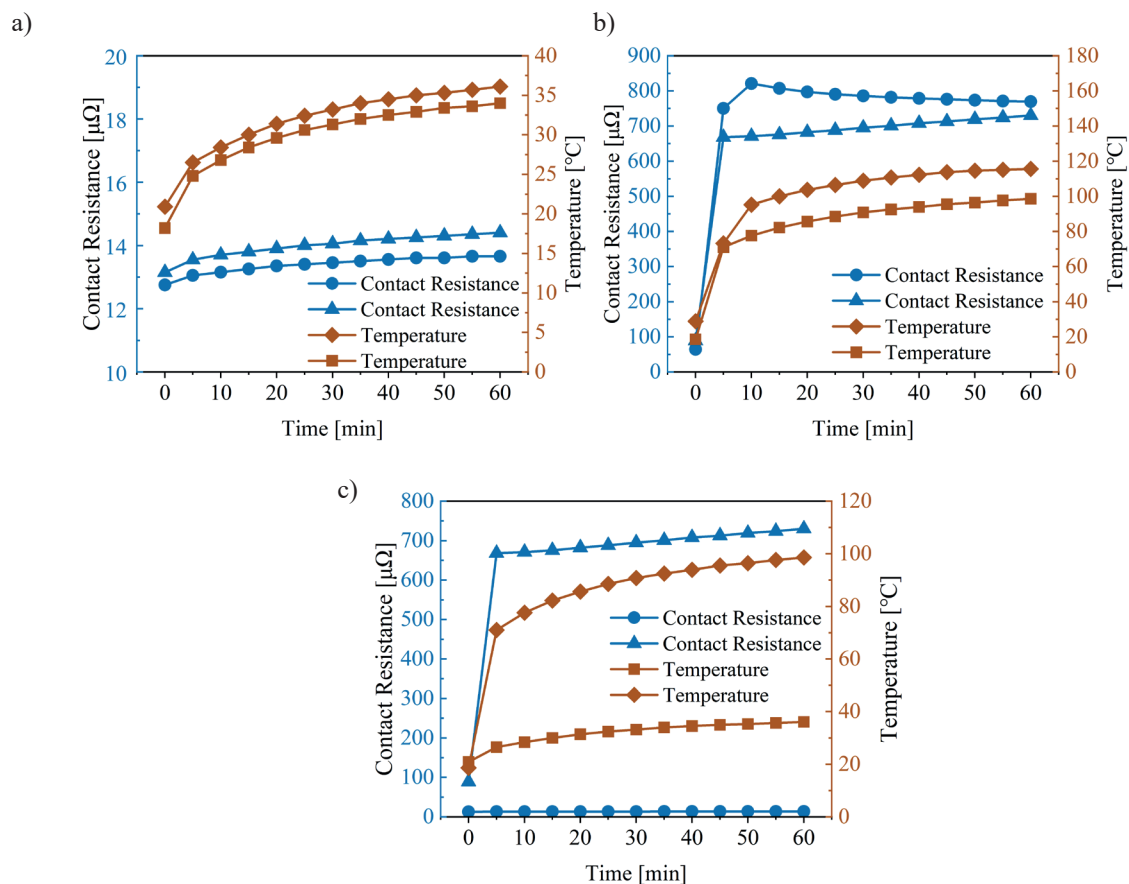


**Fig. 6.** Cross-comparison experimental results: a) dynamic test results under the same nickel-plated aluminum busbar; b) dynamic test results under the same bare aluminum busbar; c) dynamic test results under the same copper busbar

### 4.3. Equivalent conductive area analysis based on Holm's contact theory

While the electrical connectors are in contact, the actual conductive contact area is often much smaller than the nominal or theoretical contact area (Aronstein, 2004; Oberst, 2021). The actual contact area can be estimated indirectly from the measured contact resistance. According to Holm's electrical contact theory, the contact resistance can be expressed as:

$$R = R_c + R_f = \frac{\rho_1 + \rho_2}{4a} + \frac{\sigma}{\pi a^2} \quad (1)$$

where:  $R$  – contact resistance;  $R_c$  – constriction resistance;  $R_f$  – film resistance;  $\rho_1, \rho_2$  – resistivities of the contacting materials; and  $a$  – radius of the conductive spot.

To estimate the size of the actual conductive contact region, the real contact area is considered as a large composite circular region composed of several discrete small contact spots. Since electricity is generally conducted in conjunction with the rupture of non-conductive films, the radius of the hypothetical composite conductive region,  $a$ , can be calculated as (Braunovic, 2003; Oberst et al., 2018):

$$a = \frac{\rho_1 + \rho_2}{4R} \quad (2)$$

By taking  $\rho_1 = \rho_{Al} = 2.82 \times 10^{-8} \Omega \cdot m$  and  $\rho_2 = \rho_{Sn} = 1.09 \times 10^{-7} \Omega \cdot m$ , the radius  $a$  can be determined. The actual contact area can then be estimated using the area formula for a circle. The calculated results are presented in Tab. 4.

The results confirm that in copper–bare aluminum connectors under current flow, the actual conductive area is very small. Moreover, the conductive area  $A_c$  decreased noticeably before and after dynamic testing, indicating that electrical conduction was primarily car-

ried by a limited number of micro-protrusion contact spots. The current paths at the interface were highly localized, and the constriction resistance was highly sensitive to the characteristic dimensions of these contact spots. Consequently, the formation or destruction of even a few microcontacts can lead to significant fluctuations in contact resistance.

### 4.4. Mechanism of contact resistance dynamic evolution

In summary, based on a multidimensional analysis of sample surface morphology changes, interfacial compositional changes, and variations in actual contact area, combined with the results of cross-comparison experiments, the dynamic evolution mechanism of contact resistance in copper–bare aluminum electrical connectors under dynamic testing conditions is illustrated in Figure 7. Without surface treatment, the naturally formed aluminum oxide layer on the aluminum busbar surface exhibits high insulation and stability. Under the applied contact force, only a very limited number of effective metal contact spots are formed in local high-pressure regions during initial assembly, and these restricted conductive pathways constitute the initial low contact resistance state.

During dynamic testing, under the coupled effects of current, temperature, and contact pressure, the contact interface undergoes a series of changes. On the one hand, the softer tin-plated layer on the copper busbar undergoes significant plastic deformation, resulting in a substantial decrease in surface roughness. On the other hand, high current and the increase in temperature significantly accelerate further oxidation of the aluminum busbar surface, with newly formed aluminum oxide rapidly covering and electrically isolating the previously established metal contact spots.

**Table 4.** Estimated contact area results

ID	$A_{c1}$ [mm <sup>2</sup> ]	$A_{c2}$ [mm <sup>2</sup> ]	$A_m$ [mm <sup>2</sup> ]	$A_{c1}/A_m$ [%]	$A_{c2}/A_m$ [%]
1	8.701	0.00631	455.51	1.910	0.00138
2	12.407	0.00691	455.51	2.724	0.00152
3	11.208	0.00699	455.51	2.461	0.00153
4	12.336	0.00787	455.51	2.708	0.00173
5	0.864	0.00622	455.51	0.189	0.00137
6	0.311	0.00889	455.51	0.068	0.00195
7	0.843	0.00590	455.51	0.185	0.00129
8	2.184	0.00624	455.51	0.479	0.00137
9	2.631	0.00585	455.51	0.577	0.00129
10	1.509	0.00694	455.51	0.331	0.00152

Notes:  $A_{c1}$  – real contact area before dynamic testing;  $A_{c2}$  – real contact area after dynamic testing;  $A_m$  – nominal contact area

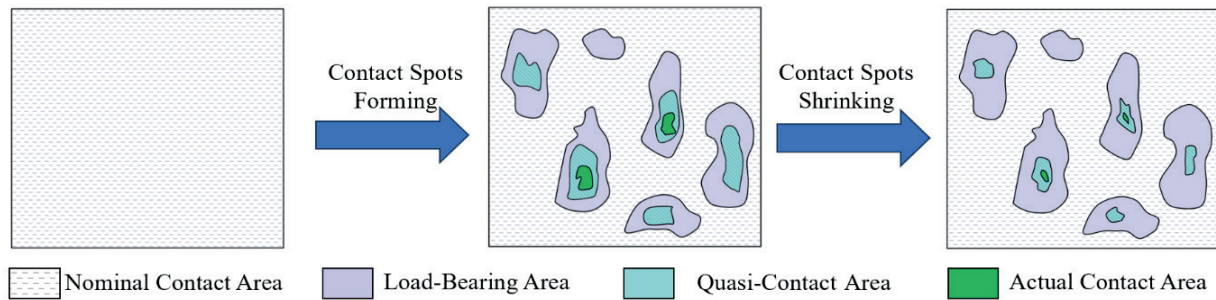


Fig. 7. Evolutionary process of the contact area

Although morphological changes on the copper busbar tend to increase the contact area, the continuous growth and coverage of the aluminum oxide layer dominate the electrical behavior of the interface, leading to a progressive reduction or even blockage of effective conductive pathways. As a result, the contact resistance exhibits an “initially low → rapid increase → gradual stabilization” trend. The final stabilized state corresponds to a dynamic equilibrium between oxide growth and local breakdown (or partial conduction).

This mechanism indicates that in copper–bare aluminum contact systems, the dynamic behavior of the aluminum surface oxide layer is the key factor determining contact resistance stability. Without effective suppression or modification of the oxide layer, the interfacial electrical contact performance is unlikely to be maintained over the long term.

## 5. Conclusion

This study systematically investigated the evolution of contact resistance and the reliability of copper–aluminum electrical connectors in automotive lithium-ion batteries. Static contact resistance measurements, dynamic current tests, and microscopic characterization analyses were carried out to identify the key factors influencing contact resistance, reveal the dynamic evolution behavior under continuous current conditions, and uncover the governing mechanisms based on analyses of surface morphology, surface elemental composition,

and relevant theory. The main conclusions are summarized as follows:

- The factors significantly affecting the contact resistance of copper–aluminum electrical connectors are aluminum busbar plating, contact force, and sample hardness. Nickel plating of the aluminum busbar can effectively reduce and stabilize contact resistance.
- The nickel-plated aluminum busbar assemblies maintain stable contact resistance under 100 A, 200 A, and 300 A conditions. In contrast, bare aluminum busbar assemblies exhibit a pronounced increase in contact resistance under all tested current conditions, with the evolution characterized by an “initially low → rapid increase → gradual stabilization” trend.
- After dynamic testing, the evolution of the contact interface in copper–bare aluminum connectors exhibits pronounced asymmetry. On the copper busbar, the primary changes are plastic deformation and planarization of the tin-plated layer, whereas the aluminum busbar undergoes more substantial oxide layer thickening and coverage. The combined effects of both sides determine the interfacial contact state, with the dynamic behavior of the aluminum oxide layer playing a decisive role in the observed increase in contact resistance.

## Acknowledgments

The authors would like to acknowledge the financial support from the Gotion High-Tech Endowed Chair for Lightweight Technology of Battery System.

## References

- Alderete, B., Nayak, U. P., Mücklich, F., & Suarez, S. (2023). Influence of topography on electrical contact resistance of copper-based materials. *Surface Topography: Metrology and Properties*, 11(2), 025027. <https://doi.org/10.1088/2051-672X/11/2/025027>
- Aronstein, J. (2004). An updated view of the aluminum contact interface. In *Proceedings of the 50th IEEE Holm Conference on Electrical Contacts and the 22nd International Conference on Electrical Contacts. Electrical Contacts – 2004* (pp. 98–103). IEEE. <https://doi.org/10.1109/HOLM.2004.1353101>

- Bao, Y.-f., Ren, L., Yu, Z.-t., Jiang, Y.-f., & Yang, K. (2018). An experimental study on contact resistance of coated galvanized steel sheet. *Welding in the World*, 62(3), 511–516. <https://doi.org/10.1007/s40194-018-0583-9>
- Braunovic, M. (2003). Effect of connection design on the contact resistance of high power overlapping bolted joints. *IEEE Transactions on Components and Packaging Technologies*, 25(4), 642–650. <https://doi.org/10.1109/TCAPT.2003.809108>
- Elkjaer, A., Ringen, G., Bjørge, R., Hagen, C. H. M., Lædre, S., & Magnusson, N. (2022). Reliability of bolted aluminum busbars for battery systems: effect of nickel coating and corrosive environment. *IEEE Transactions on Transportation Electrification*, 9(1), 1060–1071. <https://doi.org/10.1109/TTE.2022.3196309>
- Feng, Y., Ding, Y., Mao, Z., Hu, X., Wang, Z., Huang, C., & Ye, C. (2021). Research on the Protective Performance of Tinning Layer on Electrical Copper Bars. *Materials Protection*, 54(06), 112–116. <https://doi.org/10.16577/j.cnki.42-1215/tb.2021.06.020> [in Chinese].
- Hu, M., Ye, Z., Liu, Q., Lv, Q., & Wang, L. (2019). Cause analysis and solution of quality problems of Tin plating layer on copper wiring head. *Electric Locomotives & Mass Transit Vehicles*, 54(06). <https://doi.org/10.16212/j.cnki.1672-1187.2019.06.018> [in Chinese].
- Huang, W., Xia, N., & Tian, S. (2022). Study on reliability of deep sea lithium battery connection mode. *Marine Electric & Electronic Engineering*, 42(04), 28–30+33. <https://doi.org/10.13632/j.meee.2022.04.011> [in Chinese].
- Kalich, J., Matzke, M., Pfeiffer, W., Schlegel, S., Kornhuber, L., & Füssel, U. (2022). Long-term behavior of clinched electrical contacts. *Metals*, 12(10), 1651. <https://doi.org/10.3390/met12101651>
- Khayam, U., Sutrisno, B., Risdiyanto, A., & Suwarno (2014). Design of battery connection using copper conductor with tin and silver coating. In *2014 International Conference on Electrical Engineering and Computer Science (ICEECS)* (pp. 326–330). IEEE. <https://doi.org/10.1109/ICEECS.2014.7045271>
- Khayam, U., Hadisoeseo, N. P. Y., Suwarno, & Risdiyanto, A. (2017). Reducing contact resistance of high current connectors on electric vehicle by controlling contact pressure and addition of plating material. In *2017 4th International Conference on Electric Vehicular Technology (ICEVT)* (pp. 61–64). IEEE. <https://doi.org/10.1109/ICEVT.2017.8323534>
- Kolmer, P., Shukla, A., & Song, J. (2022). Methods of material and surface analysis for the evaluation of failure modes for electrical connectors. *Technologies*, 10(6), 124. <https://doi.org/10.3390/technologies10060124>
- Oberst, M., Schlegel, S., & Gromann, S. (2018). Influence of oxygen on the aging of electrical joints with one bare and one coated aluminum contact member. In *2018 IEEE Holm Conference on Electrical Contacts* (pp. 262–269). IEEE. <https://doi.org/10.1109/HOLM.2018.8611688>
- Oberst, M., Hildmann, C., & Schlegel, S. (2021). Deterioration and Breakdown Mechanisms in force-fitted current-carrying Connections between Aluminum and Tin. In *2021 IEEE 66th Holm Conference on Electrical Contacts (HLM)* (pp. 1–7). IEEE. <https://doi.org/10.1109/HLM51431.2021.9671165>
- Runde, M. (2019). Inside the aluminum contact spot. In *2019 IEEE Holm Conference on Electrical Contacts* (pp. 1–8). IEEE. <https://doi.org/10.1109/HOLM.2019.8923842>
- Slade, P. G. (Ed.). (2017). *Electrical Contacts: Principles and Applications* (2nd ed.). CRC Press.
- Song, J., Yuan, H., Shukla, A., Koch, Ch., & Hilmert, D. (2019). Correlation of connector contact failures in accelerated testing and in long-term use field vehicles. In *2019 IEEE Holm Conference on Electrical Contacts* (pp. 296–302). IEEE. <https://doi.org/10.1109/HOLM.2019.8923844>
- Song, J., Hilmert, D., & Kiel, F. (2025). Mechanisms of failure and state analysis of electrical connectors in automobiles. *Engineering Failure Analysis*, 173, 109427. <https://doi.org/10.1016/j.engfailanal.2025.109427>
- Taheri, P., Hsieh, S., & Bahrami, M. (2011). Investigating electrical contact resistance losses in lithium-ion battery assemblies for hybrid and electric vehicles. *Journal of Power Sources*, 196(15), 6525–6533. <https://doi.org/10.1016/j.jpowsour.2011.03.056>
- Tian, N. (2019). *Sliding Contact Characteristics and Reliability Analysis of Different Contact Materials of Connector* [Master's thesis, Beijing University of Posts and Telecommunications] [in Chinese].
- Wu, Q. (2017). *Fretting Contact Characteristics and Reliability Analysis of Contact Pairs of Different Coating Materials* [Master's thesis, Beijing University of Posts and Telecommunications] [in Chinese].
- Zhang, C., Ren, W., & Liao, X. (2022). On the relationship between contact resistance and load force for electrode materials with rough surfaces. *Materials*, 15(16), 5667. <https://doi.org/10.3390/ma15165667>
- Zhang, S., Zhao, X., Ye, M., & He, Y. (2019). Theoretical and experimental study on electrical contact resistance of metal bolt joints. *IEEE Transactions on Components, Packaging and Manufacturing Technology*, 9(7), 1301–1309. <https://doi.org/10.1109/TCPMT.2019.2920854>
- Zhi, H. (2016). *Experimental Study of Electrical Contact Characteristics for Aviation Electrical Connector under Combined Environmental Stress* [Master's thesis, Harbin Institute of Technology] [in Chinese].
- Zhu, Z. (2023). *Study on Low Cost and High Performance Precious Metal Composite Electrical Contact Coating* [Doctoral dissertation, University of Science and Technology Beijing]. <https://doi.org/10.26945/d.cnki.gbjku.2023.000100> [in Chinese].